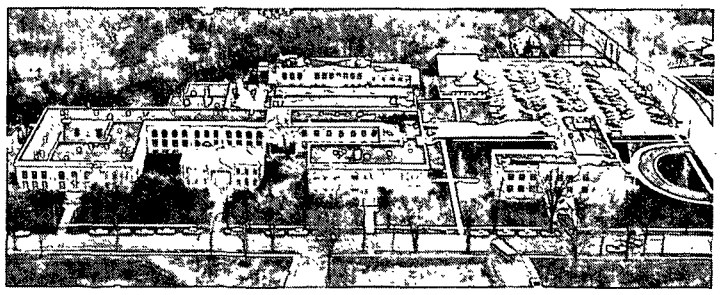

THE INSTITUTE OF PAPER CHEMISTRY, APPLETON, WISCONSIN

IPC TECHNICAL PAPER SERIES

NUMBER 324

STRATEGIES FOR END-USE PERFORMANCE

GARY L. JONES

FEBRUARY, 1989

Strategies for End-Use Performance

Gary L. Jones

This manuscript is based on results obtained in IPC research and is to be presented at the TAPPI Contaminant Problems and Strategies in Waste Paper Recyling Seminar on April 24-26, 1989 in Madison, WI

STRATEGIES FOR END-USE PERFORMANCE

Gary L. Jones
The Institute of Paper Chemistry
Appleton, WI 54912

ABSTRACT

Simulation of the effects of repulping fibers on sheet properties showed good agreement with previous experimental results. Agreement was obtained by adjusting the apparent fiber stiffness factor which in turn reduced bond density. The results showed that refining alone cannot restore properties to those of virgin fibers because of the irreversible effects such as fines generation and reduced fiber length. Mild chemical treatments which restore fiber flexibility but do not affect freeness or fines content appear to be the best means of reversing the effects of hornification on drying.

BACKGROUND

It is now well-known that repulping dried fibers results in reduced bonding in the reformed sheet. As a result, tensile and bond-sensitive properties such as Z-D tensile are significantly reduced. The effects of repulping vary with species and densification conditions, i.e., refining and pressing.

McKee (1971) showed that for an unspecified southern pine kraft pulp, refined to 325 CSF and made into British handsheets, each repulping led to a decrease in density, breaking length, burst, bonding strength, and bonded area. Zero-span tensile also decreased with repulping. Variables such as tear and Taber stiffness factor increased. The behavior was strong evidence of network debonding. Although the rate of change of properties with each repulping appeared to drop, there did not appear to be any evidence of a leveling off in properties after many repulpings.

Bobalek et al. (1988) subsequently demonstrated similar effects for five different furnishes for three repulpings but under significantly less severe densification conditions, i.e., higher CSF and zero wet pressing pressure. Bobalek did not see the same change in sheet density as seen by McKee. Zero-span tensile increased with repulping indicating that actual bond development was continuing with refining in the absence of pressure. This behavior probably reflects the low level of bonding present in the initial sheets.

Consistent with McKee's findings, breaking length, Z-D tensile and Scott Bond decreased, indicating reduced bonding. Repulping under very mild conditions appeared to have little effect on printing properties such as opacity, scattering coefficient and Parker print surface.

Klungness (1974) showed that the effects of repulping on fiber and network properties are not so much caused by contaminants but by the deinking and repulping processes used to remove the contaminants. He also found strong evidence of a reduction in fiber bonding. Fiber bonding and sheet strength could be restored to essentially their virgin fiber values by the repulping processes, i.e., PE removal and deinking.

A review of recent technologies in the field of secondary fiber reuse has been compiled by TAPPI Press (Hamilton et al. 1988).

Until recently, process simulation was limited to mass and energy balances and provided no useful information on the effects of secondary fiber reuse on end-use performance of paper. This predictive capability is now available with the Performance Attribute System of MAPPS (Modular Analysis of Pulp and Paper Systems), a process simulation package developed at The Institute of Paper Chemistry.

Because the PAT system is relatively new, there have been few detailed evaluations of the system. Simulations of a hypothetical TMP mill illustrated the potential applications of the system (Jones 1988a). The simulation predictions in a TMP mill were shown to be in reasonable agreement with actual measurements (Jones 1988c). A full mill case study is currently underway to verify other parts of the model system.

OBJECTIVE

This work was undertaken to demonstrate that a simulation program could predict the effects of repeated pulpings on fiber and sheet properties and indirectly validate the understanding in the models. It was also hoped that this work could suggest ways of reversing property degradation on repulping.

PROCEDURE

A kraft flowsheet model was developed with MAPPS to predict the flows, attributes and properties of the virgin kraft pulp for each of the species of interest, longleaf pine, aspen, and jack pine and a 50/50 mixture of aspen and jack pine. The process included a kraft digester, a staged brownstock washing system, a screening, cleaning and reject refining system, chlorine and hypochlorite bleaching and extraction stages and a final atmospheric refining stage.

Flows of black and white liquor to the digester were adjusted so each species was cooked to the same yield and kappa. Power and/or consistency to the final refining stage was adjusted to achieve the desired freeness. Comparisons were made with McKee's data at a CSF of 325 and 60 psi wet pressing pressure assuming the species to be longleaf pine. Similar comparisons were made with the data of Bobalek et al. at zero psi pressure and a variety of freeness levels for aspen, northern pine and a 50/50 mixture of aspen and northern pine.

The simulation then continued onto the paper machine where sheets were formed. The paper machine flowsheet consisted of a fourdrinier model containing a gravity drainage zone, a series of foils and suction boxes followed by a wet press section, a drier section and a saveall system. The output of this flowsheet was a dry sheet with asso-

ciated attributes and sheet properties.

However, the dewatering and sheet consolidation behavior in the paper machine simulation differed considerably with each species as might be expected. The equilibrium level of fines and retention on the wire also varied with species. This required adjustments of vacuum pressures, press loadings and drier conditions to achieve a similar sheet dryness. Formation index varied with average fiber length which in turn influenced final sheet properties.

This indicated that significant differences between handsheet and machine made properties would be predicted. Interpretation of the response to repulping and comparisons to the data would become more difficult if paper machine operation were included in the analysis. Therefore, to limit the scope, the handsheets were returned directly to a point before the final refiner in the kraft mill. Handsheet properties were estimated at each repulping cycle and compared with the data of McKee and Bobalek et al.

Figure 1 shows the process flowsheet. The Kraft Mill and Paper Machine blocks represent MAPPS flowsheets described above.

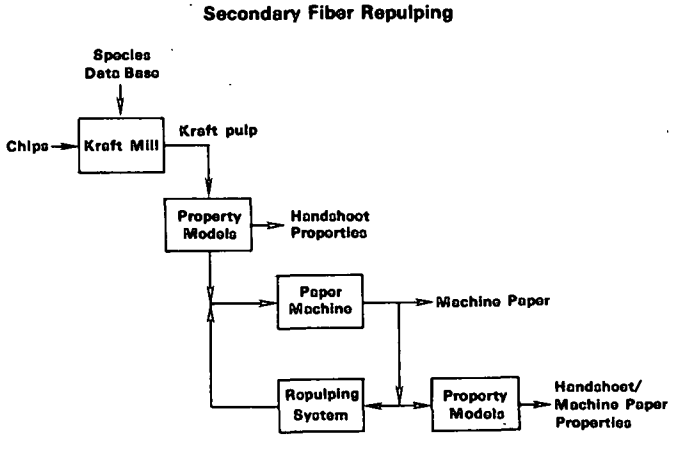

Figure 1. Repulping process flowsheet.

A complete discussion of the Performance Attribute System is beyond the scope of this work. It is anticipated that portions of this system will be described in upcoming publications. The current discussion is limited to aspects relating to network bonding, sheet density and the effects of fiber and sheet properties and processing conditions on handsheet properties. The portion of the PAT system relevant to the current discussion is shown in Appendix I.

The effect of repulping is simulated by increasing stiffness parameter, SF, with each repulping. Inspection of the equations for sheet density, effective bond density and sheet tensile properties shows how SF influences these properties. Because the effects are quite complex, several representative variables are shown in Figures 2 through 8 over the range of conditions covered in the McKee and Bobalek data.

DISCUSSION OF RESULTS

Table 1 summarizes the repulping conditions. Tables 2 and 3 compare the simulation results with the data of McKee and Bobalek et al., respectively, for virgin pulp and for multiple repulpings. The results for intermediate repulpings were intermediate to those shown. Numbers 1 through 16 in Table 1 refer to conditions shown in Figures 2 through 5.

Table 1. Conditions used in repulping experiments.

	Freeness, mL	Pressure, psi	No. of Repulpings
1	606	60	0
2	606	60	6
3	606	0	3&6
4	606	1000	6
5	554	60	0
6	554	0	0
7	554	60	6
8	486	60	0
9	486	0	0
10	407	0	0
11	407	60	0
12	407	60	6
13	337	0	0
14	337	60	0
15	337	60	6
16	486	0	3&6

For the McKee data, the relative change in all variables except tear factor are accurately predicted. Taber stiffness is predicted to increase somewhat more than the data indicate. The agreement is good considering the uncertainty in reproducing the conditions used in preparing the British handsheets used in the tests. All the trends indicate that bonding decreases with increased number of repulpings. The stiffness factor varied from 1 to 1.5.

Table 2. Relative change in handsheet properties of repeated repulping comparison with McKee data.

CSF: 337 mL Yield: 47% Long Leaf Pine Pressure: 60 psi

	Virgin Fiber Simulation	Six Repulpings Simulation	% Change Data	% Change Simulation
Density, g/cc	0.80	0.712	-13	-11
Breaking length, km	10.35	7.88	-29	-24
Stretch, %	2.4	1.94	-19	-19
Burst factor	80.1	50.7	-38	-37
Tear factor	--	--	+23	--
Scattering, cm^2/g	227	302		+33
Taber stiffness factor	0.026	0.032	+15	+23
Z-tensile, GPA	0.65	0.50	-21	-23
Porosity, sec/100 mL	32.6	21.8	-33	-33

Table 3 compares the results of zero and three repulpings on selected properties. Note that CSF was not reproduced exactly in the simulations. There is reasonably good agreement between the data and simulation values and the trends are also predicted reasonably well with the exception of the breaking length for the mixture of jack pine and aspen. As with the McKee data, the simulations were based on increasing stiffness factor during the drying step. After three repulpings SF was equal to 1.25.

Table 3. Comparison with data of Bobalek & Chaturvedi.

Yield: 47% Pressure: 0 psi

	No. of Repulpings	Wt. Avg. Fiber Length, mm		CSF, mL		Sheet Density, g/cc		Breaking Length, km		Light Scattering Coef., m^2/kg		Z-D Tensile GPA	
		D	S	D	S	D	S	D	S	D	S	D	S
Aspen	0	1.2	1.0	550	486	0.26	0.27	1.6	1.7	41	45.4	0.23	0.364
	3	1.1	1.0	540	486	0.29	0.31	1.5	1.9	40	44.8	0.18	0.328
% Change						+12	+15	-6	+11	+2	+1	-22	-10
Jack Pine	0	3.2	2.4	600	601	0.22	0.23	2.1	2.0	32	47.3	0.24	0.41
	3	3.4	2.4	600	601	0.23	0.27	1.7	2.5	29	46.8	0.18	0.36
% Change						+5	+17	-19	+20	-9	-1	-25	-12
50/50 Jack Pine/ Aspen	0	2.0	1.9	590	520	0.23	0.23	2.0	2.0	35	47.2	0.19	0.40
	3	2.0	1.9	580	580	0.26	0.275	1.9	2.5	34	46.7	0.18	0.36
% Change						+13	+20	-5	+20	-3	-1	-5	-10

The increase in sheet density upon repulping and the general increase in tensile and decrease in scattering coefficient indicate that additional bond formation is occurring with the mild refining used during each repulping stage. However, the sharp decrease in both TEA (not shown) and Z-D tensile indicate a decrease in bonding. These results differ from those of McKee in part due to the zero wet pressing pressures used to make the handsheets.

These differences are illustrated in Figures 2 through 8. The response to refining and to repulping is quite different at low wet pressing pressures. Sheet density increases with refining (decreasing CSF) and wet pressing pressure. Density is predicted to decrease with repulping (stiffer fibers) at 60 psi pressure and to increase with repulping at lower pressures and low levels of refining.

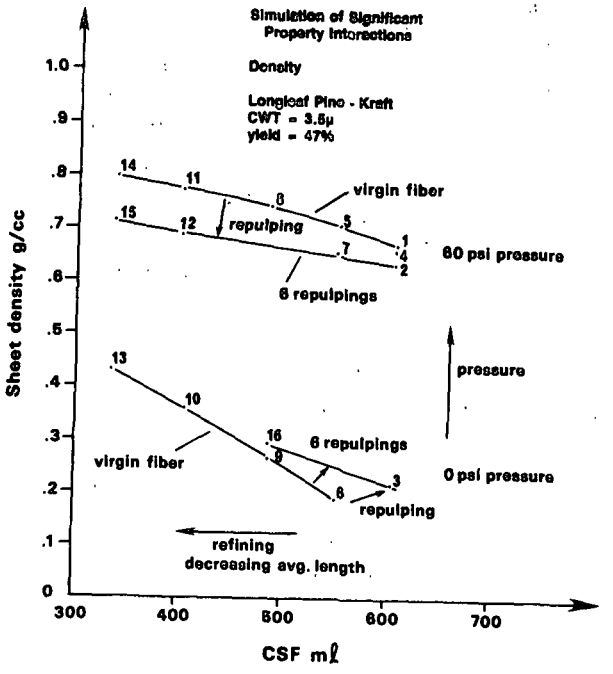

Figure 2. Sheet density.

Figure 3 shows that the relationship between breaking length and density varies with the level of refining, pressing and repulping. Refining and pressure shift the curves upward, while repulping shifts the curve downward at higher pressure and laterally at lower pressure. The response is similar for burst factor shown in Figure 4.

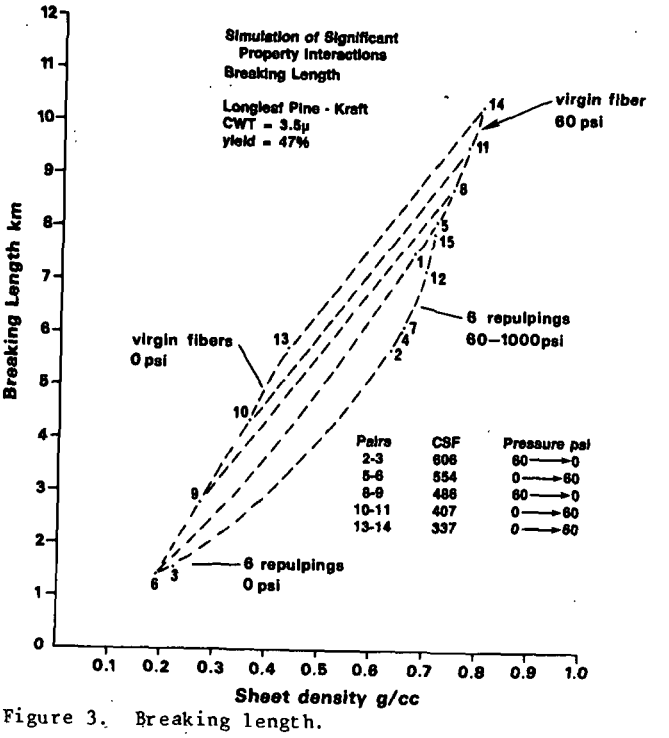

Figure 3. Breaking length.

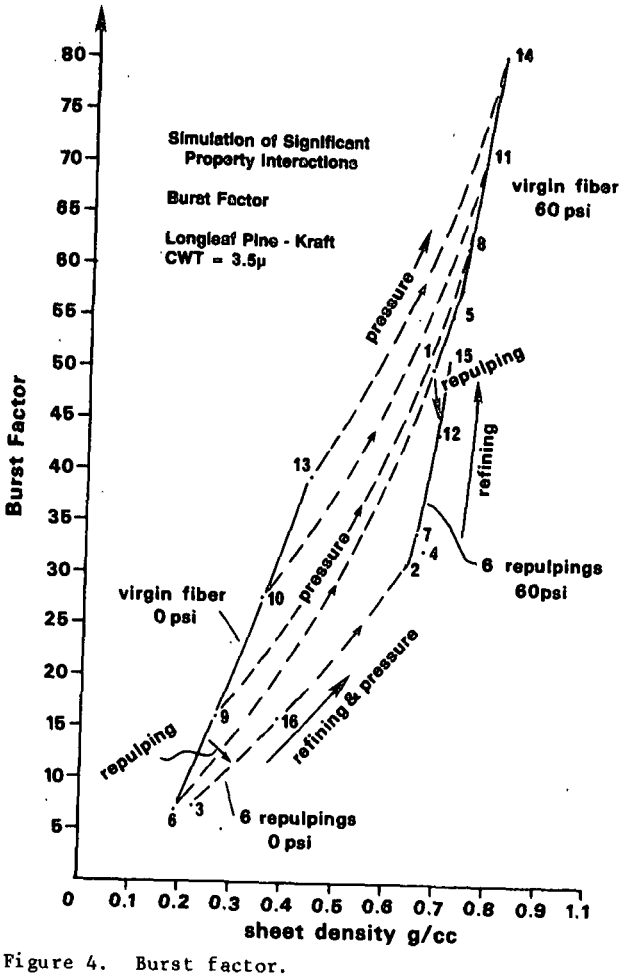

Figure 4. Burst factor.

The tear factor (Figure 5) response tends to be the opposite of breaking length. However, tear is very responsive to changes in fiber length and much less responsive to changes in pressure. Increased refining reduces tear in two ways: by reducing fiber length and by increasing density or other tensile properties. Repulping and higher pressure shifts the line to lower densities while the reverse is predicted at lower pressures.

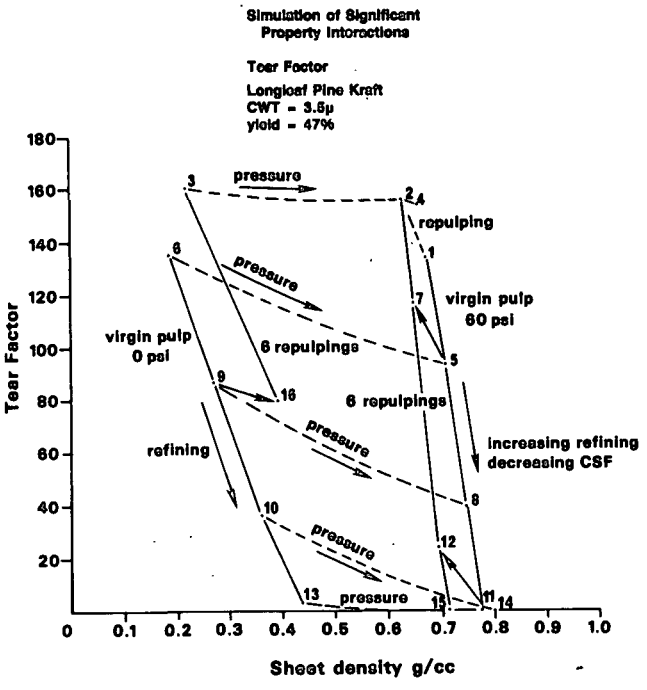

Figure 5. Tear factor.

Scattering coefficient (Figure 6) decreases with increasing density. The entire response is shifted to higher scattering for a given density as a result of repulping. The absorption coefficient was computed to be 5 cm^2/g for all species because of the similarity in pulped kappa and yield. Brightness predicted from Kubelka-Munk theory varied from 80 at point 14 to 86 at point 6 in general agreement with McKee's data. However, brightness was predicted to increase slightly with repulping.

Z-D tensile (Figure 7) is predicted to decrease with increasing densification at lower densities and to increase with increasing densities at higher densities. However, the upturn at densities below 0.3-0.4 is counter-intuitive and may not be correct. Although it is stated in the literature that Z-D tensile is a measure of bonding, there is conflicting evidence of its relationship to bonding.

The data of Bobalek et al. indicate that while sheet density increases by 5 to 13% in the low density range, Z-D tensile decreases by 5 to 25%. The data used to develop the Z-D tensile model from Fleischman (1982) do not go below a sheet density of 0.4 g/cc. Therefore, the upturn at low densities is a result of extrapolating a nonlinear correlation. A followup study should determine if this effect occurs at low density.

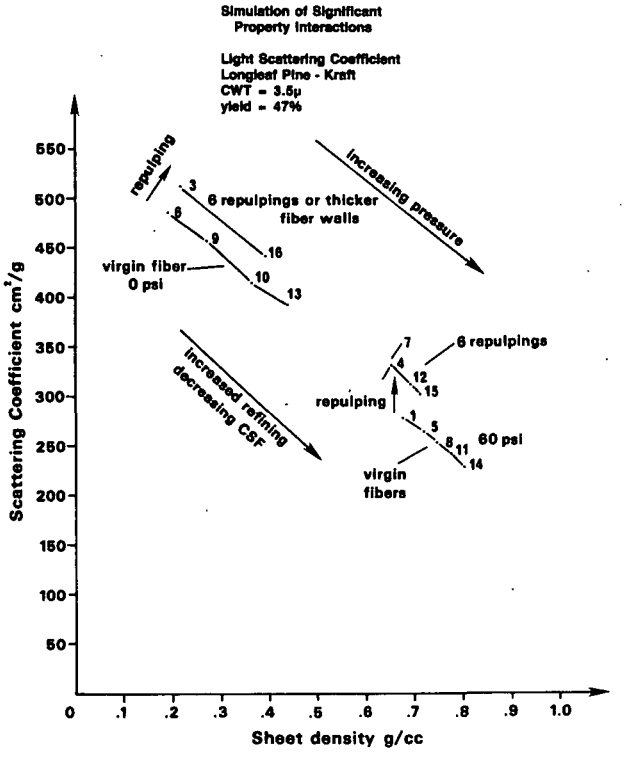

Figure 6. Scattering coefficient.

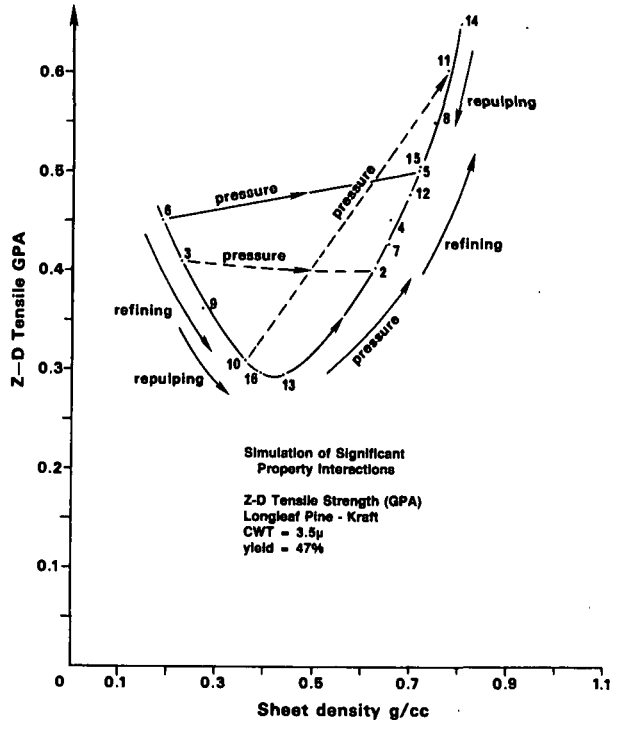

Figure 7. Z-D tensile.

Taber stiffness factor shown in Figure 8 behaves very much like scattering coefficient despite the highly nonlinear dependence on sheet density. Repulping is predicted to have little effect at

higher density and tends to decrease at lower density. Repulping also reduces the slope making TS less sensitive to both pressure and refining at higher levels of repulping.

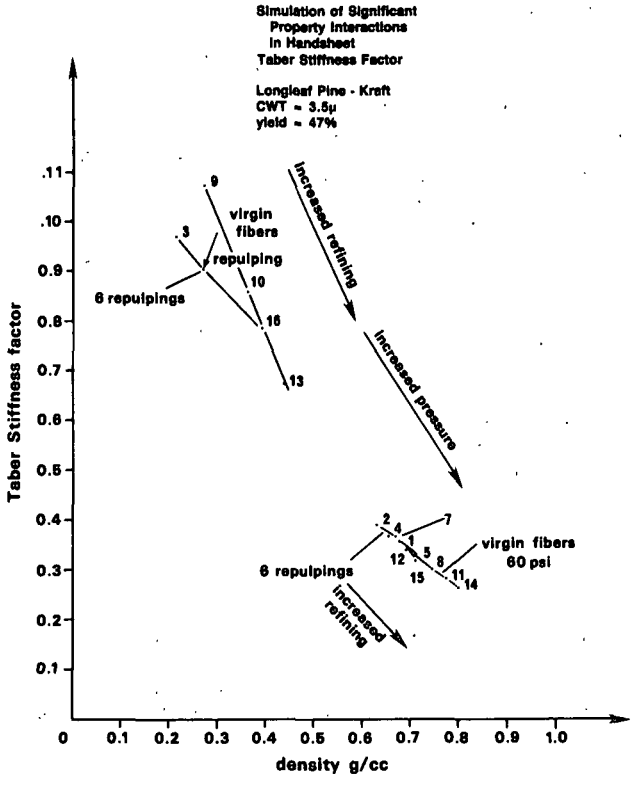

Figure 8. Taber stiffness.

CONCLUSIONS

The simulations show that models used in the performance attribute system provide useful and reasonably accurate estimates of the many effects of repulping, refining and wet pressing for a number of species. The primary factors which influence properties from virgin fibers are shown to be intrinsic fiber tensile strength, CSF, yield, wet pressing pressure, cell-wall thickness and fiber length. Stiffness factor enters in only after fibers are dried.

Many of the effects of repulping can be modeled by an apparent increase in fiber stiffness which has the effect of increasing cell wall thickness. The reduction in tensile properties with repulping can be partially reversed by refining. However, other properties such as tear factor will also change irreversibly.

Mild chemical treatments which restore fiber flexibility but do not affect freeness or fines content appear to be the best means of reversing the effects of hornification on drying.

ACKNOWLEDGMENTS

The author wishes to express his appreciation to the members of The Institute of Paper Chemistry for their support of this work.

REFERENCES

Alexander, S. D., Marton, R., McGovern, S. D. "Effect of Beating and Wet Pressing on Fiber and Sheet Properties II. Sheet Properties." Tappi 51(6): 283-288(1968).

Bobalek, J. F., Chaturvedi, M. "The Effect of Recycling on the Physical Properties of Specific Fibers and Their Networks." Proc. 1988 TAPPI Pulping Conference, Book 1 1988:183-187.

Clarke, J. d'A. "Factors Influencing Apparent Density and its Effect on Paper Properties. TAPPI Tech. Assoc. Papers 26: 499(1943).

Daugy, L. "A Study of Some Physical Characteristics of Mixtures of Pulps from White Oak and Poplar." M.S. Thesis, State University College of Forestry, Syracuse U., 1964.

Dinwoodie, J. M. "The Relationship Between Fiber Morphology and Paper Properties. A Review of Literature." Tappi 48(8): 440(1965).

Fleischman, E. H., Baum, G. A., Habeger, C. C. "A Study of the Elastic and Dielectric Anisotropy of Paper." Tappi J. 65(10): 115-118(1982).

Hamilton, F.; Leopold, B., eds. Pulp and Paper Manufacture, Third Edition Vol. 3, Secondary Fibers and Non-Woven Pulping, jointly published by TAPPI and CPPA, 1988.

Han, S. T. "Compressibility and Permeability of Fibre Mats." Pulp Paper Mag. Can. 70: T134(1968).

Jones, G. L. "Simulating the Development of Pulp and Paper Properties in Mechanical Pulping Systems." Pulp Paper Can. 89(6): 128(June, 1988).

Jones, G. L. "MAPPS Performance Attributes Simulation." Progress Report No. 1, Project 3471, The Institute of Paper Chemistry, March 25, 1988b.

Jones, G. L. "Simulation of the Performance Characteristics of a TMP Mill." 1988 Process Simulation Symposium, CPPA, Quebec City, QUE, CANADA, Sept., 1988c.

Klungness, J. H. "Recycled Fiber Properties as Affected by Contaminants and Removal Processes." Tappi 57(11): 71-75(1974).

McKee, R. C. "Effect of Repulping on Sheet Properties and Fiber Characteristics." Paper Trade J. 155(21): 34-40(May 24, 1971).

Nissan, A. H., Batten, G. L., Jr. "Unification of Phenomenological, Structural and Hydrogen-Bond Theories of Paper, Using Percolation Concepts." Nordic Pulp and Paper Research J. 8-14 (1987).

Onogi, S., Sasaguri, K. "The Elasticity of Paper and Other Fibrous Sheets." Tappi 44(12): 874 (1961).

Page, D. H. "A Theory for the Tensile Strength of Paper." Tappi 52(4): 674(1969).

Page, D. H., Seth, R. S., and De Grace, J. H. "The

Elastic Modulus of Paper. I. The Controlling Mechanisms." Tappi J. 62(9): 99(1979).

Robertson, A. A. and Mason, S. G., Tappi 33(6): 403 (1950).

Strand, B. D. and Edwards, L. L. "Optimum Design, Operation and Control of Mechanical Pulping Systems." Tappi J. 67(12): 72-5(1984).

Yan, J. F. "Kinetic Theory of Mechanical Pulping." Tappi J. 58(7): 156-8(1975).

NOMENCLATURE

BL	breaking length, km
BF	burst factor, kPa m^2/g
C33	stiffness, GPa
CO	consistency, %
CSF	Canadian Standard Freeness, mL
CWT	cell-wall thickness, microns
E	elongation at break, %
FS	stiffness factor, dimensionless
FRM	formation factor, dimensionless
K	K-factor, dimensionless
L	average length, mm
LCUM	cumulative distribution function
NSP	net specific power, hsp-ton/day
OR	orientation ratio
P	pressure, psi
RE	rupture energy, ergs
S	normalized surface or bond area
SCC	scattering coefficient, cm^2/g
T	absolute temperature, K
TF	tear factor, mN m^2/g
TS	Taber stiffness factor
WS	wet strength, %
X	weight fraction
Y	yield, %
YM	Young's modulus, GPa
ZI	intrinsic fiber breaking length, km
ZZ	Z-D tensile, GPa

Greek

ρ	density
Σ	summation

Subscripts

a	actual (bonded area)
b	potential
e	effective
h	hydrodynamic
i	inlet
l	lower
m	moisture
u	upper

APPENDIX I

Portions of the MAPPS Performance Attribute System relevant to the effects of repulping on sheet properties. Derivations may be found in a report to the members of The Institute of Paper Chemistry (Jones 1988b).

Sheet Density Model

The sheet density model was developed from the data of Alexander and Marton (1968 a and b).

Sheet Density

$$1/\rho = 1/\rho_u + (1/\rho_l - 1/\rho_u)\ (1/S_b^2)$$

where the upper asymptotic limit to density, ρ_u is given by,

$$\rho_u = 1/(0.764 + 0.000477\ CSF + 0.1146\ CWT\ SF)$$

where CWT is the fiber cell wall thickness, microns. CWT, CSF and Y collectively represent factors which influence fiber flexibility and bonding. SF, the stiffness factor, represents the effect of drying on fiber flexibility. In predried fibers, SF equals one. The effects of drying and repulping are simulated by increasing SF with each drying step.

Under the experimental conditions, ρ_u varied between 0.65 and 0.95.

ρ_l represents the low limit to the sheet density, i.e., unbonded sheet density.

$$\rho_l = 1/(1/\rho_u + 43.14 + 0.08726\ Y - 0.05866\ CSF)$$

ρ_l varies from 0.05 down to 0.13. The following limit condition is placed on ρ_l.

$$\rho_l > \rho_{lim}$$

$$\rho_{lim} = 0.05\ (CWT\ SF - 0.8) + 0.002\ (Y - 48)$$

Hydrodynamic specific surface was found to be a linear function of CSF. Robertson and Mason (1950) found essentially the same relationship for kraft pulps.

$$S_h = 95.7 - 0.012\ CSF$$

The potential bonded area before wet pressing, S_{bi}, is proportional to S_h.

$$S_{bi} = S_c \quad S_h$$

where S_c represents the fraction of total external surface which bonds. S_c decreases with increasing yield.

$$S_c = 0.0734 - 0.000654\ Y$$

For a yield of 48%, S_c is 0.042, indicating 4.2% bonding. For example at 700 CSF, S_h is 10 and S_{bi} is 0.42 m^2/g. At 100% yield, S_c is 0.008 indicating only 0.8% of the total surface is bonded.

The result of wet pressing at pressure P is to increase S_b from S_{bi} according to the Han concept,

$$S_b = S_{bi}\ (1 + M\ P^N)$$

where M and N are functions of CSF and Y.

$$M = e^{(0.14414 + 0.00127\ CSF)}$$

$$N = 0.0003\ CSF - 0.000015\ Y$$

Compressibility decreases with decreasing yield and CSF.

CSF is related to fiber length distribution through

the K-factor model of Strand and Edwards (1984).

$$CSF = e^{(7 - 0.33\ A)}$$

where A is related to the discrete weight-average fiber length distribution function X_i and K by

$$A = 1 - (1/K)\ \Sigma\ X_i\ \ln(L_i/2.4)$$

L_i is the average length for length range i. K accounts for differences in surface area development due to the uniformity and extent of refining, species and pulping on external fibrillation.

For a primary refiner

$$K = K_0 = 1.54\ e^{((0.123 - 0.0237\ CO)\ NSP)}$$

For secondary or reject refiners K depends on K_0 in addition to net specific power, NSP, and refiner inlet consistency, CO, %.

$$K = K_0\ e^{(k_2\ NSP)}$$

and

$$k_2 = -\ 0.598 + 0.088\ NSP/K_0 - 0.05\ K_0\ CO$$

The weight average fiber length distribution function is determined by the average and standard deviation and distribution type specified in the species data base or independently by the user. The fiber length and width distributions during refining are based on Yan's kinetic model.

Assuming fiber length can be described by a log-normal distribution, the weight-average fiber length L and standard deviation in the discharge of a refiner (or beater) is a function of the inlet, L_i as follows,

$$L = A_1 + (L_i - A_1/A_2)\ e^{(-A_2\ ZP)}$$

$$\sigma_L = A_1 - A_2/L$$

where ZP is the power function defined by Yan (1975).

$$ZP = 10^{(NSP - 76.7)/41.7)}$$

Coefficients A_1, A_2, may be changed to reflect changes in species, refiner plate design, etc. The fiber/bundle width distribution is detemined in a similar way.

Fiber length distribution function X_i is defined as the difference between cumulative distribution functions for fiber length, L_i, $LCUM_i$ and fiber length L_{i-1}, $LCUM_{i-1}$,

$$X_i = LCUM_i - LCUM_{i-1}$$

$$X_1 = LCUM_1$$

$LCUM_i$ is defined in terms of the error function, $erf(ZL_i)$ with argument ZL_i which is a function of L_i and the average and standard deviation of the distribution.

$$LCUM_i = 0.5\ (1 + erf\ (ZL_i))$$

$$ZL_i = \ln(L_i - S_3)/S_1 - S_2$$

$$S_1 = \sqrt{2}\ \ln(\sigma_L)$$

$$S_2 = S_1/2$$

$$S_3 = \ln\ (XLG)$$

$$XLG = L\ \ e^{(-1.5\ \ln\ \sigma^2)}$$

L_i are average values of length for each screen fraction.

The number average fiber/bundle width distribution functions are defined in a similar fashion.

Potential bonded area, S_b represents the area in optical contact. On drying, hydrogen bonds are formed and S_b is converted to actual bonded area, S_a according to the work of Nissan and Batten (1987).

$$S_a = S_b\ e^{(-(X_m + 0.0024\ (T - 25))}\quad X_m < 0.045$$

$$S_a = S_b\ e^{(-(6.4\ X_m - 0.2433 + 0.0024\ (T - 25))}$$

for $X_m > 0.045$.

Effective Bond Density

The effective bond density also depends on formation factor. It is assumed that formation factor is unity for handsheets.

$$\rho_e = \rho_a\ FRM$$

where ρ_a is actual bond density or ρ defined above for $S_b = S_a$.

Actual Bond Density

$$1/\rho_a = 1/\rho_u + (1/\rho_1 - 1/\rho_u)\ (1/S_a^2)$$

Fiber Stiffness Factor

Fiber stiffness factor increases during drying as a result of the conversion of potential to actual bonded area.

$$FS = FS_i(\ 1 + 1.083\ S_a/S_b)$$

where FS and FS_i are the outlet and inlet stiffness factors, respectively. FS is equal to one initially.

For a sheet with ideal formation, FRM equals 1. When dried to maximum dryness, ρ_a equals ρ and sheet properties are directly related to sheet density. However, situations which affect bonding but apparently have little effect on bulk density are accounted for by the decoupling of bulk density from effective bond density.

Portions of the PAT system controlling fiber separation and mixing, interconversions from fiber flows and distribution functions, reduction in absorption coefficient and other factors are omitted.

Models for a selected set of sheet properties are described to illustrate the effect of repulping on end-use performance. The effect is simulated by

increasing SF, the stiffness factor. Because SF occurs with CWT, an increase in SF produces the same effect as an increase in cell wall thickness. Sheet tensile properties are defined in terms of effective bond density, ρ_e. Breaking length and elastic modulus models are based on work of Page (1969, 1979).

Sheet breaking length (km):

$$BL = Z\ (\rho_e - 0.098)/(0.5\ \rho_e + 1)$$

where Z is related to intrinsic fiber strength. It is proportional to zero-span tensile.

$$Z = ZI - 1.88\ CWT\ SF$$

For very highly bonded sheet zero-span approaches ZI. For normal bonding ZI is larger than zero-span. ZI must be chosen to fit the overall behavior for a given species. As SF increases with repulping, Z and BL decrease. ρ_e usually decreases with repulping at normal wet pressing pressures. However, it may also increase at low levels of bonding (high CSF and low P).

Young's Modulus, YM, 10^{10} dynes/cm^2:

$$YM = E_f\ (\rho_e - 0.1719)$$

E_f, fiber modulus, is set to 10.7.

Elongation at Break, %:

$$E = 0.852 + 0.2677\ BL - 0.1771\ YM$$

Burst Factor, BF (standard units) is given by the Van den Akker model:

$$BF = b\ E^{1/2}\ BL$$

where b depends on fiber stiffness, species and refining.

$$b = 5.625 - 0.1266\ CWT\ SF\ (1 + 0.0015\ CSF)$$

Rupture energy, RE, 10^3 ergs is proportional to breaking length.

$$RE = 219(\ BL - 2.6)$$

Tear Factor, TF, (used for yields less than 85%) increases with wt.-avg. fiber length and decreases with increased bonding represented by elongation at break and burst factor.

$$TF = 38.5\ L - 0.435\ E\ BF$$

Scattering Coefficient, SCC, cm^2/g, depends on optical contact between fibers but is assumed to be independent of formation or the presence of actual bonds.

$$SCC = S_u - 430.68\ (\rho - \rho_l)$$

$$S_u = 636.6 - 2.613\ Y$$

Z-D tensile, ZT, depends on effective bond density, average fiber orientation, OR, and wet stretch, WS, %. These are set to 1 and 1, respectively, for random handsheets. The directional property models were developed from original data taken by Fleischman et al. (1982).

$$ZZ = 0.2204 + 1.86\ C_{33}$$

where C_{33} is the stiffness in the Z direction,

$$C_{33} = 0.30778 - 1.252\ 10^{-3}\ \rho_e + 1.436\ 10^{-6}\ \rho_e^2 +$$

$$1.15\ 10^{-5}\ \rho_e\ OR + 2.95^{-5}\ \rho_e\ WS$$

Taber Stiffness Factor, TS, is proportional to Young's modulus divided by bond density to the third power.

$$TS = 2 \times 10^{-3}\ YM/\rho_e^3$$